International Journal of Heat and Mass Transfer 116 (2018) 194–207

Contents lists available at ScienceDirect

International Journal of Heat and Mass Transfer

journal homepage: www.elsevier.com/locate/ijhmt

Thermal performance of peripheral-finned tube evaporators under frosting

Marco A.S. Timmermann [a], Massoud Kaviany [b], Jader R. Barbosa Jr. [a,*]

[a] Polo - Research Laboratories for Emerging Technologies in Cooling and Thermophysics, Department of Mechanical Engineering, Federal University of Santa Catarina, Florianópolis, SC 88040900, Brazil

[b] Department of Mechanical Engineering, University of Michigan, Ann Arbor, MI 48109, USA

ARTICLE INFO

Article history:
Received 29 May 2017
Received in revised form 29 July 2017
Accepted 2 September 2017
Available online 17 October 2017

Keywords:
Peripheral finned-tube
Frost formation
Heat transfer enhancement
Heat exchanger

ABSTRACT

This study presents an experimental and theoretical evaluation of frost formation on the moist air side of a peripheral finned-tube (PFT) heat exchanger. Previous studies of this compact geometry correlated the friction and heat transfer parameters above the dew-point temperature of the air (no frost or condensate formation). Here, for the first time, the thermal-hydraulic performance of a PFT heat exchanger is analyzed under frosting. A PFT heat exchanger prototype was evaluated experimentally in a closed-loop wind tunnel calorimeter to determine the influence of the tube wall temperature, air velocity and psychrometric properties (temperature and relative humidity) on the heat transfer rate, air-side pressure drop and frost buildup on the surface. The thermal and hydrodynamic behavior of the enhanced air-side surface was analyzed using a distributed heat exchanger model in which mass, momentum and energy balances are applied to one-dimensional control volumes in the air flow direction. The model treats the air flow path as a porous medium in which the porosity, equivalent particle diameter and thermal properties vary as a function of time due to the frost accumulation. Good agreements (within 20% average error) between the model predictions and the experiments for the air-side pressure drop and heat transfer rate have been found. The enthalpy effectiveness was found to drop from 0.68 for dry to 0.50 under severe frosting, which suggests that the PFT heat exchanger continues to be effective under frost.

1. Introduction

Frosting is an undesirable yet inevitable occurrence in some refrigeration and air-conditioning equipment. Different from ice, which is the result of freezing of water vapor condensate, frost originates from the desublimation of water vapor from moist air flowing over solid surfaces with temperatures below the freezing point of water. Frosting diminishes the cooling capacity and the coefficient of performance (COP) of the cooling unit by adding a low thermal conductivity resistance to the air-side surface of the evaporator, which also decreases the air flow rate due to the narrowing of the air flow passages.

Frost formation can be delayed by mechanical or chemical treatment of the heat transfer surface in order to reduce the surface energy and increase the subcooling degree required for the onset of nucleation [1,2]. Slippery liquid-infused porous surfaces [3], magnetic slippery icephobic surfaces [4] and electrically conductive surface coatings [5] have been developed to repel or mitigate ice and frost formation. In refrigeration equipment, Joule heating is still the most common defrosting method (particularly in household systems), although several other techniques have been proposed (ultrasonic vibration, desiccant dehumidification, hot gas reverse cycle, etc.), as reviewed recently by Ref. [6].

An interesting complementary approach to any kind of frosting, icing and condensation prevention technique is the formulation of enhanced air-side geometries in such a way that the frost or condensate would appear at preferential locations (e.g., flow stagnation regions) where their accumulation would be less detrimental to the air flow distribution through the tube-fin matrix. The peripheral finned tube (PFT) concept developed by Ref. [7] consists of six radial fins connected at their tips by peripheral fins, as shown in Fig. 1. The hexagonal arrays are fabricated in three different sizes according to the length of the radial fins (R_1, R_2 and R_3), and are arranged around the tube with an offset angle of 30° from their neighbors, forming a structured porous medium with interconnected pores. The air flows perpendicularly to the tubes. In an evaporator, the solid surfaces are colder around the tubes, so they will naturally have a bigger tendency to accumulate frost or condensate. In the PFT geometry, those regions are

* Corresponding author.
E-mail address: jrb@polo.ufsc.br (J.R. Barbosa Jr.).

http://dx.doi.org/10.1016/j.ijheatmasstransfer.2017.09.008
0017-9310/

Nomenclature

A	area [m^2]
b	slope of enthalpy-temperature interpolation [J kg^{-1} K^{-1}]
c_p	specific heat capacity [J kg^{-1} K^{-1}]
d_p	equivalent particle diameter [m]
f	friction factor [–]
$\mathcal{G}$	convective mass transfer conductance [kg m^{-2} s^{-1}]
h	moist air enthalpy [J kg^{-1}]
h_f	fictitious enthalpy potential [J kg^{-1}]
h_g	enthalpy of ice [J kg^{-1}]
$\hbar$	heat transfer coefficient [W m^{-2} K^{-1}]
$\hbar_{oc}$	effective air-side heat transfer coefficient [W m^{-2} K^{-1}]
k	thermal conductivity [W m^{-1} K^{-1}]
K_c	contraction coefficient [–]
K_e	expansion coefficient [–]
L	length [m]
Le	Lewis number [–]
m	fin parameter [m^{-1}]
$\dot{m}$	mass flow rate [kg s^{-1}]
M	mass [kg]
N	number of fin arrays [–]
p	perimeter [m]
P	pressure [Pa]
$\dot{Q}$	heat transfer rate [W]
t	fin thickness [m]
t	time [s]
T	temperature [°C]
u	in situ air velocity [m s^{-1}]
u_D	Darcian air velocity [m s^{-1}]
UA	overall thermal conductance [W K^{-1}]
$\dot{V}$	moist air volumetric flow rate [m^3 s^{-1}]
w	fin width [m]
x	distance [m]

Greek

δ	frost layer thickness [m]
ϵ	porosity [–]
ϕ_{in}	relative humidity [–]
η_F	fin efficiency [–]
η_o	overall surface efficiency [–]
ω	humidity ratio [–]
ρ	density [kg m^{-3}]

Subscripts and superscripts

a	dry air
b	bare tube
B	fin base
c	coolant
cs	cross section
CV	control volume
F	metallic fin
g	ice
in	inlet
LM	log mean
o	air-side
out	outlet
p	peripheral fin
r	radial fin
s	frost
t	total

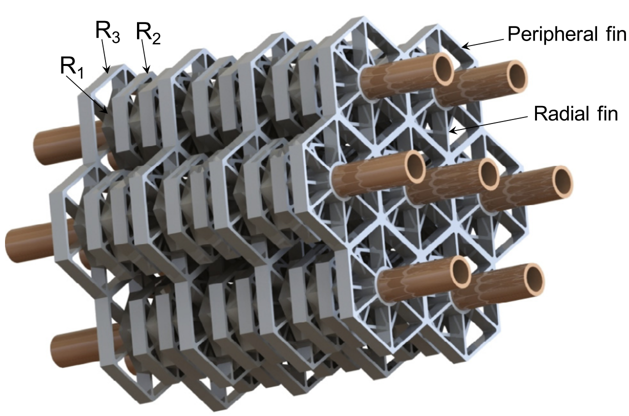

Fig. 1. The peripheral finned-tube geometry.

flow stagnation zones, so the air flow would be less disturbed by the frost growth, and would be more easily redistributed through alternative paths through the porous matrix. According to Ref. [7], the anisotropy of the porous structure also facilitates condensate drainage.

Pussoli et al. [8] performed the first experimental work on PFT heat exchangers. Five prototypes with different values of radial fin length, fin distribution and number of tube rows were tested in an open-loop wind tunnel under 'dry' conditions (no frost or condensate formation). A model to calculate the fin and overall surface efficiencies based on analytical expressions for the fin temperature [7] was integrated with one-dimensional energy and momentum balances (distributed modeling approach) to compute the air-side pressure drop and air temperature in the flow direction. Good agreement between the model and the experimental data was obtained using the particle-diameter Nusselt number correlations of Whitaker [9] and Handley and Heggs [10] and friction factor relationships due to Ergun [11] and Montillet et al. [12]. Later, Pussoli et al. [13] combined entropy generation minimization with single-phase convection performance evaluation criteria (fixed geometry, fixed face area and variable geometry) [14] to determine the optimal characteristics of PFT heat exchangers.

Generally speaking, the frosting literature can be divided into studies on (i) the measurement and correlation of physical properties [15–18], (ii) the mechanisms of frost nucleation, growth and densification [19–21], and (iii) the prediction of the performance of heat exchangers under frosting [22–25]. In the latter category, the proposed distributed models are such that the air-side flow path can be divided into one-dimensional (lengthwise) or two-dimensional (lengthwise and spanwise) control volumes onto which mass, momentum and energy balances are applied to calculate the local rates of frost formation (vapor desublimation), heat transfer and the pressure drop. The local rates are integrated over the entire area of the heat exchanger to give the overall instantaneous rates. Moreover, in two-dimensional approaches, it is possible to evaluate more precisely the influence of the refrigerant flow distribution and predict the zones of the air-side surface that are more affected by the frost accretion, which has a direct impact on the air flow distribution [22,23]. Thermal capacity effects of the frost layer are usually neglected with satisfactory results in